Received: 4 September 2021 | Revised: 5 November 2021 | Accepted: 29 November 2021

DOI: 10.1002/rra.3918

RESEARCH ARTICLE

WILEY

# Japanese knotweed increases soil erosion on riverbanks

Rébecca Matte[1] | Maxime Boivin[2] | Claude Lavoie[1]

[1]École supérieure d'aménagement du territoire et de développement régional, Université Laval, Québec City, Québec, Canada

[2]Département des sciences humaines et sociales, Université du Québec à Chicoutimi, Saguenay, Québec, Canada

**Correspondence**
Claude Lavoie, École supérieure d'aménagement du territoire et de développement régional, Université Laval, Québec City, Québec, Canada.
Email: claude.lavoie@esad.ulaval.ca

**Funding information**
Fonds Québécois de la Recherche sur la Nature et les Technologies, Grant/Award Number: 253035; National Science and Research Council of Canada, Grant/Award Number: 2018-03715

## Abstract

For years, Japanese knotweed (*Reynoutria japonica*) has been suspected of accelerating riverbank erosion, despite a lack of convincing evidence. The stems of this invasive plant die back following the first autumn frosts, leaving the soil unprotected during winter and spring floods. In Québec (Canada), riverbank erosion may also be accentuated by ice during mechanical ice breakups. The objective of this study was to evaluate the influence of knotweed on riverbank erosion along a river invaded by the species, within a context of floods with ice. The elevation along 120 cross-sectional riverbank profiles, occupied or not by knotweed, was measured before and after the spring flood of 2019. On average, riverbanks occupied by knotweed had nearly 3 cm more soil erosion than riverbanks without knotweed, a statistically significant difference. Stem density also influenced erosion: the higher the density, the greater the soil loss. Certain riverside conditions, such as the slope of the riverbank or being located on an islet, interacted with knotweed, further accentuating erosion. Soil losses measured between November 2018 and May–June 2019 were particularly pronounced, but the spring flood was also exceptional, with a recurrence interval close to 50 years. On the other hand, soil loss from rivers invaded by knotweed can be expected to increase over time, as this invasive species spreads rapidly in riparian habitats.

KEYWORDS
climate change, erosion, flood, ice, Japanese knotweed, *Reynoutria japonica*

## 1 | INTRODUCTION

Plants, through their interactions with hydrological, sedimentological, and biological processes, can influence the geomorphology of watercourses (Corenblit et al., 2011; Davies & Gibling, 2009, 2010; Murray, Knaapen, Tal, & Kirwan, 2008; Murray & Paola, 2003; Schumm, 1968; Smith, 1976). A rapid change in floodplain vegetation, such as during the colonization of riverbanks by invasive plants, may impact river morphology (Corenblit et al., 2011; Rowntree, 1991). Some invaders (e.g., *Lupinus polyphyllus*, *Tamarix* spp.) create a plant cover dense enough to stabilize the riverbanks through sediment trapping, and this may eventually result in a narrowing of the river channel (Birkeland, 1996; Graf, 1978; Meier, Reid, & Sandoval, 2013; Tickner, Angold, Gurnell, & Mountford, 2001). Other plant invaders facilitate riverbank erosion. For example, the creation of a shallow network of rhizomes by an invasive species (e.g., *Arundo donax*) may result in undercutting, causing the riverbank to retreat with each flood episode (Stover, Keller, Dudley, & Langendoen, 2018). The soil may also be left bare when the stems of the invader die (e.g., *Impatiens glandulifera*), leaving the riverbanks vulnerable to erosion during subsequent floods (Greenwood, Baumann, Pulley, & Kuhn, 2018; Greenwood, Gange, & Kuhn, 2020; Greenwood & Kuhn, 2014). This may be the case for Japanese knotweed (*Reynoutria japonica* Houttuyn [*Fallopia japonica* (Houtt.) Ronse Decreane]; Polygonaceae), an invasive rhizomatous perennial whose stems die back following the first autumn frosts.

Japanese knotweed was introduced to Europe (in 1830) and North America (in the 1860s) from Japan. Since then, it has rapidly invaded the banks of rivers and lakes, wastelands, and the embankments of roads and railways (Lavoie, 2019). It is mainly found in habitats where the soil has been disturbed, particularly on riverbanks and agricultural or urban areas where trees and shrubs have been eliminated. This perennial plant grows rapidly in the spring, forming stands (clones) with high stem densities and dense rhizome networks. Although rhizomes can grow 2 or even 3 m deep, most are found within the first 50 cm of soil (Child & Wade, 2000).

A frequent assumption regarding the environmental impact of Japanese knotweed is that it increases soil erosion (e.g., Child & Wade, 2000; Invasive Species Specialist Group, 2016; Michigan Department of Natural Resources, 2012; Mummigatti, 2008; van Oorschot et al., 2017). However, there are almost no data showing that knotweed and erosion are cause and effect (Lavoie, 2017). Increased erosion is nevertheless highly plausible, as knotweed forms monospecific stands whose aerial stems senesce following the first frosts. The dead stems may be swept away during winter and spring floods, denuding the soil (Colleran, Lacy, & Retamal, 2020). Without this biomass, riverbank roughness is reduced (Hopkinson & Wynn, 2009; Thorne & Furbish, 1995). A smoother bank accelerates runoff, which may impact riverbank erosion. Furthermore, the presence of plant biomass above the soil surface buffers against the current and ice flow. If shrubs or herbaceous plants, especially grasses, have been eliminated by knotweed competition, water and ice directly contact the soil during winter and spring floods, leaving it more vulnerable to erosion. It may consequently be hypothesized that knotweed infested soils, which are bare during the winter and spring, are more likely to be eroded.

The belowground biomass of riverbanks generally comprises a complex of roots and rhizomes of various plants (herbaceous plants, shrubs, trees). Dense belowground plant biomass is advantageous for soil retention, especially if the diameters of the roots and rhizomes are small: this increases soil cohesion, while decreasing erosion risk (Gurnell, Holloway, Liffen, Serlet, & Zolezzi, 2018; Simon & Collison, 2002; Stover et al., 2018; Zhu et al., 2018). However, the roots, and especially the rhizomes, of Japanese knotweed have large diameters, ranging from 5 to 100 mm (Child & Wade, 2000). In contrast, reed canarygrass (*Phalaris arundinacea*), another abundant invasive riparian plant in North America, has much smaller roots and rhizomes, which range from 0.1 to 5 mm in diameter (Bankhead, Thomas, & Simon, 2017; Keim, Beadle, & Frolik, 1932). The interaction between vegetation and riverbank stability is complex, and a multitude of factors influence this dynamic, such as the soil type, water flow, or pore water pressure (Van de Wiel & Darby, 2007). Nevertheless, one may question whether the competitive displacement of a dense belowground biomass of fine roots less than 50 cm deep by a network of knotweed rhizomes could accelerate riverbank erosion (Colleran et al., 2020).

A recent study evaluating the impacts of Japanese knotweed on riverbank erosion was conducted along an urban watercourse in the Philadelphia area (Pennsylvania, United States; Arnold & Toran, 2018). The objective was to elucidate the influence of riparian characteristics on erosion, including vegetation type and the degree of stream incision. Incision is the vertical erosion of a river channel (Booth, 1990). After just over 9 months of monitoring (July 2015–March 2016), riparian erosion was greater in sites with knotweed than in sites with trees. On riverbanks with both knotweed and a deeply incised channel, soil loss reached 30 cm. Soil loss was only 9 cm on riverbanks with knotweed but where the channel incision was much less pronounced. Sites with knotweed and trees, or only trees, and steeply incised reaches had at most 3 cm erosion. Arnold and Toran (2018) concluded that Japanese knotweed increases riparian erosion but only in deforested riverbanks with high stream incision. However, the low number of measurements (16 erosion pins) makes it difficult to draw firm conclusions. Whether knotweed truly causes more erosion, and which riverbanks are most at risk, especially in areas with massive spring flood events and mechanical ice breakups, have yet to be answered.

The main objective of this study was to evaluate the effect of Japanese knotweed on the erosion of riverbanks subjected to recurrent floods and mechanical ice breakups. Using high-precision instruments, we measured the morphological changes of riverbanks colonized or not by knotweed following a particularly strong spring flood that occurred in 2019. We hypothesized that (a) soil erosion of riverbanks occupied by knotweed is significantly greater than that of riverbanks with an herbaceous plant cover and that (b) the steeper the riverbank slope, the greater the erosion (soil loss).

## 2 | METHODS

### 2.1 | Study area

This study was carried out along the Etchemin River, in the Chaudière-Appalaches region of southern Québec, Canada (Figure 1). This river with stable meanders is highly invaded by Japanese knotweed. Its source (46°35′16.5″N; 70°25′27.5″W) is located in the Appalachian mountain range. Its outlet is the St. Lawrence River, near the city of Lévis (46°45′47.6″N; 71°13′52.3″W). The Etchemin River is 124-km long, and its catchment area covers 1,466 $km^2$. Agricultural lands cover 30% of the catchment area, forests 61%, wetlands 4%, and urbanized areas 2% (Conseil de bassin de la rivière Etchemin, 2014). Agricultural lands, mainly cultivated for corn and soybean, are mostly concentrated downstream in the St. Lawrence River lowlands. Data recorded from 1981 to 2010 at the Beauséjour weather station, situated 8 km west of Saint-Henri-de-Lévis (Figure 1), indicate that the mean annual temperature is 4°C, January being the coldest month (mean temperature: −13°C) and July the warmest month (mean temperature: 19°C). Annual precipitation totals 1,253 mm, of which 26% fall as snow (Environnement Canada, 2021).

The mean daily discharge of the Etchemin River at Saint-Henri-de-Lévis, 9 km upstream from the outlet, was 27 $m^3s^{-1}$ between 1980 and 2018 (Ministère de l'Environnement et de la Lutte contre les changements climatiques du Québec, 2020). The months with the highest mean daily discharges were April (86 $m^3s^{-1}$) and May (45 $m^3s^{-1}$), whereas the months with the lowest were January, February, August, and September (12–16 $m^3s^{-1}$). In spring 2019, the return of temperatures above 0°C and abundant precipitation caused a particularly strong flood, which began by April 14. The flood peaked on April 20, with a flow discharge of 444 $m^3s^{-1}$ (Figure 2). The

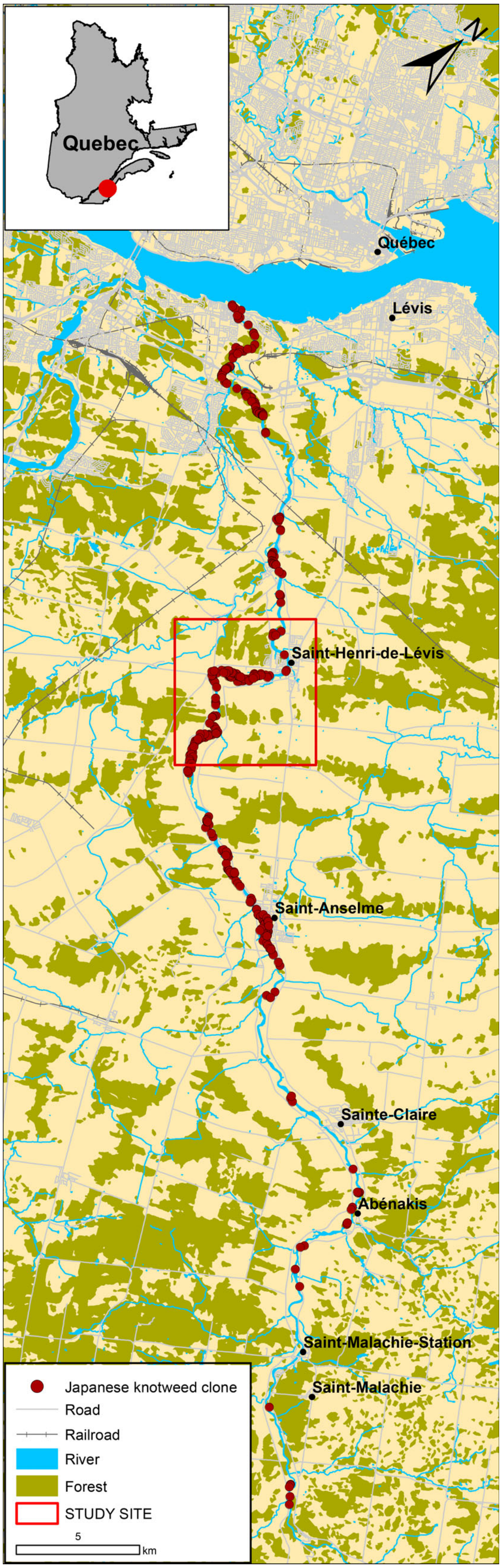


**FIGURE 1** Distribution of Japanese knotweed along the Etchemin River (Québec, Canada) in 2017. The study site was located in the village of Saint-Henri-de-Lévis [Color figure can be viewed at wileyonlinelibrary.com]

mechanical ice breakup that occurred during the spring flood resulted in an ice jam at Saint-Henri-de-Lévis that persisted a few days (Figure 3). On December 22, 2018, a sudden ice breakup also occurred, although the flow discharge was lower (215 $m^3s^{-1}$) than during the April 2019 flood event.

Data were sampled along a 15-km long section of the Etchemin River located in the municipality of Saint-Henri-de-Lévis, an agricultural community with a few residential and industrial areas. In this section, the banks of the Etchemin River are infested with numerous Japanese knotweed clones (Figure 1) that covered in 2017 a total estimated area of 86,200 $m^2$, that is, about 50% of the vegetated riverbanks (Matte, 2020). The other riverbanks are essentially covered with herbaceous vegetation.

## 2.2 | Riverbank erosion measurement

Elevation changes pre- and postflood provide an estimate of erosive soil losses at a given location. This technique is often used to measure riparian erosion and, more broadly, to document morphological changes of a channel (Bartley et al., 2008; Dietrich, 2014; Duró, Crosato, Kleinhans, & Uijttewaal, 2018; Foucher, Salvador-Blanes, Vandromme, Cerdan, & Desmet, 2017; Harmel, Haan, & Dutnell, 1999; Ziliani & Surian, 2012). Elevation changes resulting from the 2019 spring flood and ice breakup were measured with a series of cross-sectional riverbank profiles reconstructed with a differential global positioning system (DGPS). A Leica Viva GS14 DGPS (Leica Geosystems, Heerbrugg) was used for the profiles (Figure 4). This two-piece device comprised a base that was placed on a survey marker with known geographic coordinates and altitude, and a mobile antenna that was moved between sampling points. The base and antenna communicated with each other by radio communication for real-time kinematic survey mode. Data acquired using this technology permitted relatively high-precision (±8 mm) measurements of elevation at the same points (±8–15 mm) before and after the 2019 spring flood. The advantage of this technology, compared to the use of erosion pins (sensu Arnold & Toran, 2018, and Greenwood et al., 2018), is that it can generate a very high number of sampling points (by the thousands). Furthermore, erosion pins are unlikely to remain in place when confronted with the erosive force of ice blocks during spring floods.

Twenty riverbank segments covered with Japanese knotweed, and 20 other segments without knotweed but with herbaceous plant cover, were selected for the profiles in the river section chosen for this study (Figure 5). A segment was 26-m long, that is, the median value of the distance covered by a knotweed clone along the Etchemin riverbanks in 2017 (Matte, 2020). All continuous 26-m long segments with knotweed were mapped, for a total of 45; 20 of them were then randomly selected for sampling using a random number generator. All continuous 26-m segments with herbaceous plant cover were also mapped, for a total of 106; 20 of them were then randomly selected for sampling. For each selected segment, with or without knotweed, three riverbank profiles were produced with the DGPS, for

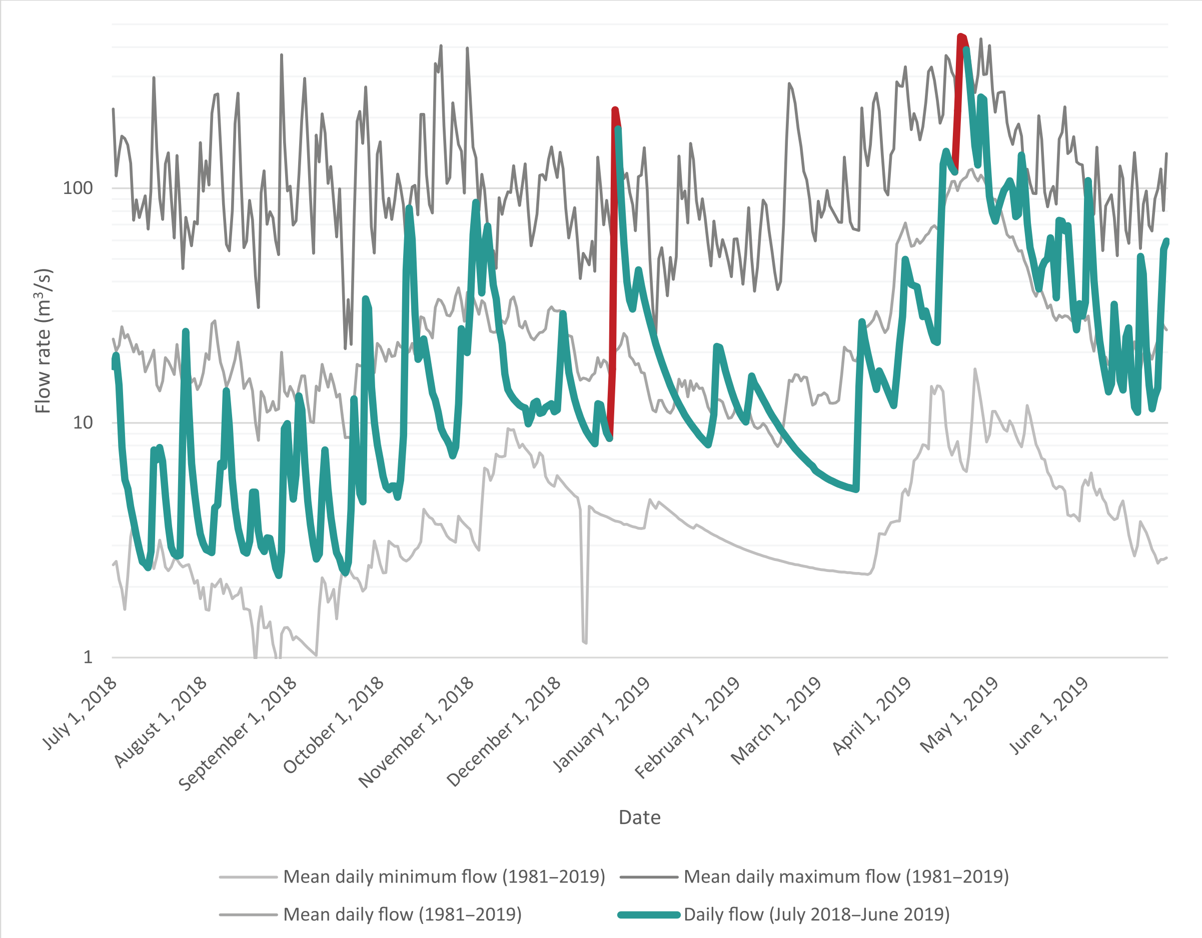


**FIGURE 2** Mean daily discharge of the Etchemin River (Québec, Canada) at the village of Saint-Henri-de-Lévis between July 2018 and June 2019 (Ministère de l'Environnement et de la Lutte contre les changements climatiques du Québec, 2020). The flood peaks, a little before January 1 and around mid-April, are indicated in red on the graph. Average discharge data for the period spanning 1981–2019 are shown for comparison [Color figure can be viewed at wileyonlinelibrary.com]

**FIGURE 3** The mechanical ice breakup that occurred during the 2019 spring flood of the Etchemin River (Québec, Canada) resulted in an ice jam at Saint-Henri-de-Lévis. This photograph, taken April 24, shows ice blocks lying on the flood plain and numerous dead Japanese knotweed stems that were ripped out by ice and water (photograph: Rébecca Matte) [Color figure can be viewed at wileyonlinelibrary.com]

a total of 120 profiles (40 segments × 3 profiles). One of the three profiles was positioned at the center of the segment, whereas the other two were positioned midway between the center and the ends. Cross-sectional profiles were generated twice, at the same points, that is, before (November 2018) and after (May–June 2019) the spring flood of 2019.

In November 2018, permanent survey markers were installed at the top of the riverbanks to ensure identical starting points in 2018 and 2019. Profiles started at the top of the riverbank and continued in the river, ending when the water was too deep for safety. Elevation sampling points used for a profile were distributed along a measuring tape installed perpendicular to the riverbank. Latitude, longitude, and elevation data were taken with the DGPS at each morphological change observed along the profile (Duró et al., 2018; Lawler, 1993). These morphological changes included depressions, sediment accumulations, or irregularities created by slope variations. Even changes of a few centimeters were recorded with the DGPS for precision. Where the riverbank had no such discontinuities over several meters, measurements were taken every 50 cm. The first DGPS dataset (pre

(a)

(b)

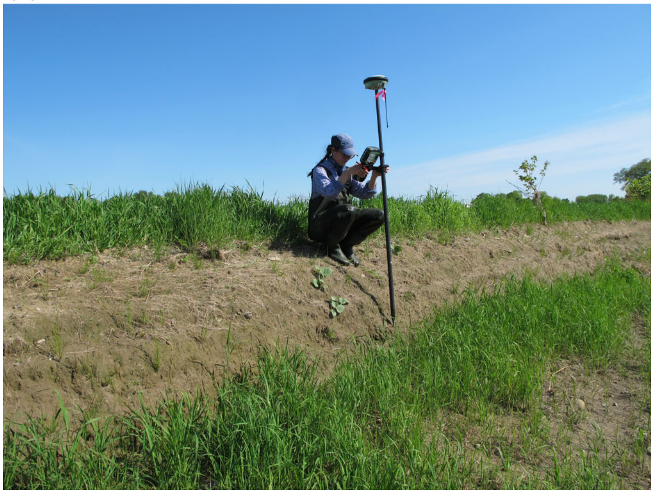

**FIGURE 4** Two riverbanks of the Etchemin River (Quebec, Canada), one with Japanese knotweed (a), the other with herbaceous vegetation (b), that were sampled with a differential global positioning system for reconstructing elevation profiles before and after the 2019 spring flood (photographs: Marianne Bouchard) [Color figure can be viewed at wileyonlinelibrary.com]

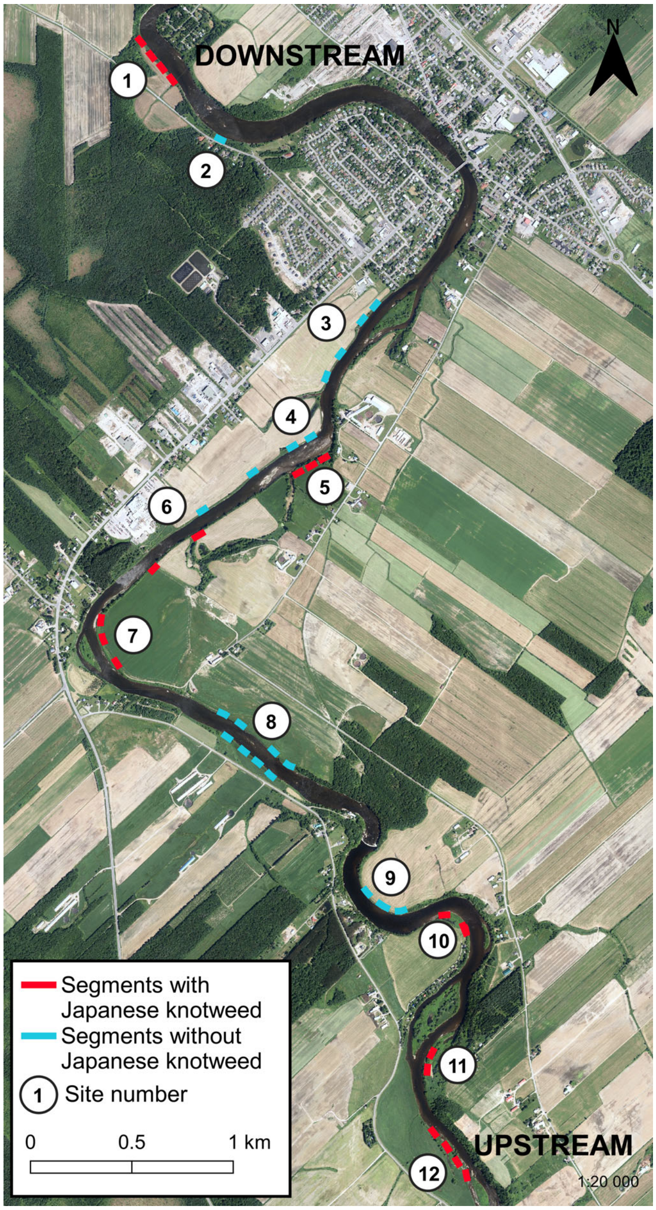


**FIGURE 5** Riverbank segments (26-m long) of the Etchemin River (Quebec, Canada), with or without Japanese knotweed, that were selected for constructing elevation profiles before and after the 2019 spring flood. Segments sharing common characteristics were grouped into sites. These comprised groups of more or less adjacent segments located along stretches of river having the same riverbank morphology [Color figure can be viewed at wileyonlinelibrary.com]

flood) was taken from November 11 to 19, 2018. The second (post flood) was taken from May 16 to June 18, 2019. Despite our best efforts, it was impossible to place the DGPS at exactly the same sampling points pre- and post flood, because in many cases, the riverbank profiles had been modified by the floods and ice flow. To obtain accurate profiles, new points were taken along the same lines (profiles) as 2018, but where new (May–June 2019) morphological changes were detected.

Because the DGPS elevation points were not taken at the exact same points along the profiles in autumn 2018 and spring 2019, data transformation was necessary to evaluate elevation changes caused by erosion. First, the position of the points (latitude and longitude) was transformed into distance from the permanent survey marker, that is, the starting point at the top of the profile. This was accomplished by importing the point data into the ArcGIS software, version 10.6 (ESRI, 2018). The interactive *Point Profile* tool from the *3D Analyst* toolbar produced the riverbank profile diagrams. The elevation data for the profile points as a function of their distance from the survey marker were then imported into Excel software (Microsoft, 2016), for autumn 2018 and spring 2019 data. In Excel, the riverbank profiles of 2018 and 2019 were overlain on diagrams (point clouds with smoothed curves). Data were then filtered to only retain points lying between the marker at the top of the riverbank and the water level of June 2019. To determine the elevation changes between the two sampling periods, the elevation values for spring 2019 were subtracted from those of autumn 2018. A positive result indicated an accumulation of sediment, whereas a negative result indicated erosion. Given that the DGPS points taken in November 2018 and May–June 2019 were not positioned at the exact same points along the profiles, an Excel matrix was constructed to interpolate the elevation between measured points, every 10 cm along the profiles. Elevation changes were calculated from these interpolated points. A total of 11,952 elevation change points were generated by this procedure.

## 2.3 | Riverbank characteristics

Riverbank erosion may be due to many factors other than Japanese knotweed. The riverbanks were therefore characterized to elucidate the impact of other explanatory variables. These variables were (a) soil textural class, (b) riverbank slope, (c) riverbank morphology, (d) the site where a riverbank segment was located, (e) riverbank vegetation, and (f) knotweed stem density.

A soil sample was taken from each riverbank segment, at the middle of each profile. The sample was extracted from the top 25-cm soil layer. Each sample was air dried and then sieved to retain particles less than 2 mm in diameter. A particle size analysis (sedimentation with dispersing agent; Bouyoucos, 1962) was conducted in the laboratory to determine the soil textural class (clay, fine silt, coarse silt, sand). The riverbank slope (%) was estimated for each profile using the initial profile points taken in November 2019. The slope was estimated for the top of the riverbank and the bank itself (water level position) by tracing a line across the profile. The closer the slope value to zero, the gentler the incline. Riverbank morphology refers to the geomorphology of the channel, that is, the shape of the river where a segment was located. In the study area, the four types of riverbank morphology were (a) linear, (b) concave, (c) convex, and (d) on an islet. The morphology of the Etchemin riverbanks was determined using aerial photographs (Ministère de l'Énergie et des Ressources naturelles du Québec, 2015).

Segments sharing common characteristics were grouped into sites. These comprised groups of more or less adjacent segments located along stretches of river having the same riverbank morphology. Grouping segments into sites permitted control, in the statistical models, of the fixed effects of location, ensuring that the observed elevation changes did not depend on intrinsic site factors. This procedure helps to decipher whether Japanese knotweed really has a significant effect on erosion, or whether it is just of a matter of coincidence, that is, that higher erosion occurred where knotweed is present simply because fluvial conditions are more forceful at those locations.

Vegetation surveys were performed from July 2 to 18, 2019. At every 1 m along a profile, from the riverbank top marker to the edge of the water, a 2-m long rod was held vertically, and each vascular plant species touching the rod was noted. Given the low species diversity, the vegetation data were later simplified into two categories, that is, (a) with Japanese knotweed or (b) without Japanese knotweed (=herbaceous vegetation). One of these two categories was then associated to each of the 11,952 elevation change points, using the data from the closest vegetation sampling point. Knotweed stem density was evaluated along the profiles using 1-$m^2$ quadrats. Stems were counted from July 12 to 14, 2019, in three quadrats per transect. The first quadrat was placed at the top of the riverbank, the second at the bottom of the riverbank, and the third midway between the first two. A stem density measurement was then associated to each of the 11,952 elevation change points, using the data from the closest knotweed sampling quadrat.

## 2.4 | Statistical analyses

A data file was created by associating each elevation change value, determined every 10 cm along the profiles, to a value for (a) soil textural class, (b) riverbank slope, (c) distance between the point and the river (minor bed; June 2019), (d) riverbank morphology, (e) segment number, and (f) site number. To test the effect of Japanese knotweed on riverbank erosion, two multiple regression analysis models were created using the least squares method (LSM). For each model, the continuous dependant variable was the elevation change in centimeters at the points before and after the 2019 spring flood. The main independent variable was knotweed, expressed in two distinct ways, that is, (a) a binary variable having a value of 1 (knotweed present) or 0 (knotweed absent) at a given point (model 1), and (b) the knotweed stem density per square meter (continuous variable) at a given point (model 2). The six other explanatory variables were included in the models to control for sampling site characteristics; segment number and site number were used to test the fixed effects of location. The models were corrected with White's method (White, 1980) to account for heterogeneity of variance (heteroscedasticity) and to ensure the validity of the significance tests. The variance was modeled by site. In addition to the two basic models, four additional models were built using two randomly drawn samples (the database was divided in half) to test the robustness of the results. Statistical analyses were conducted with Stata software (StataCorp, 2016).

# 3 | RESULTS

## 3.1 | Riverbank erosion measurement

A total of 8,111 points were taken using the DGPS along the 120 riverbank profiles, that is, 3,707 in autumn 2018 and 4,404 in spring 2019. The DGPS technology made it possible to accurately render the profiles, both in November 2018 and May–June 2019 (Figure 6). In 2019, erosion predominated over sediment deposition. Erosion, that is, negative changes in elevation with respect to November 2018, was observed at 56% of the elevation change points, and this percentage was higher for points with Japanese knotweed (66%) than for points

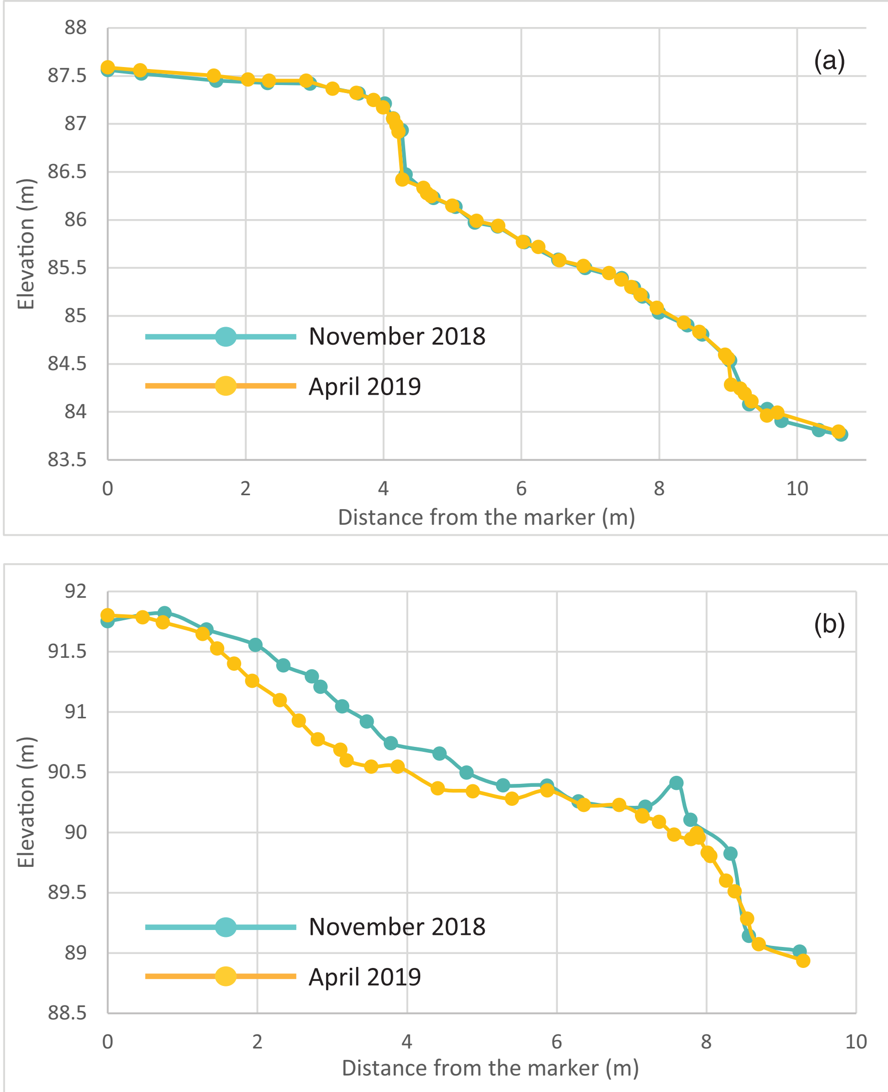


**FIGURE 6** Two examples of consecutive Etchemin River (Québec, Canada) riverbank profiles (November 2018, June 2019), without (a) and with (b) Japanese knotweed [Color figure can be viewed at wileyonlinelibrary.com]

without (49%). On riverbanks with knotweed, heavily eroded bare soil was observed at many places in spring 2019 (Figure 7). The elevation changes for points with Japanese knotweed were −4.4 cm (mean value) and −2.0 cm (median value); they were −1.8 cm (mean) and +0.1 cm (median) where knotweed was absent. The means of the elevation changes for these two vegetation categories were significantly different (*t*-test; $p < .0001$).

## 3.2 | Riverbank characteristics

The banks studied along the Etchemin River had similar soil textural classes, which varied between sandy loam (63% of the segments), loamy sand (25%), and loam (12%). The mean riverbank slope was 33% and ranged from 14% to 80%. The mean riverbank slope was 29% where Japanese knotweed was present, and 35% where it was absent. Riverbank morphology was linear along 20 segments (50%), convex along 12 segments (30%), and concave along four segments (10%). Four other segments (10%) were along islets. Knotweed had a

**FIGURE 7** Riverbank of the Etchemin River (Québec, Canada) in spring (April). When knotweed is present, the soil may be completely denuded and show obvious signs of erosion (photograph: Claude Lavoie) [Color figure can be viewed at wileyonlinelibrary.com]

much stronger presence on the islets than on the linear riverbanks (Table 1).

As expected, there were major differences in vascular plant species associated with vegetation survey points with or without Japanese knotweed (Table 2). Riverbanks with Japanese knotweed are, by far, dominated by this species. Riverbanks without Japanese knotweed are dominated by grasses, in particular reed canarygrass and smooth brome (*Bromus inermis*), two exotic rhizomatous species (Figure 4). The presence of knotweed was associated to 4,858 (41%) of the 11,952 points of elevation changes calculated for the models. The mean stem density of Japanese knotweed on the invaded riverbanks was 41 per m$^2$, ranging from 5 to 213 stems per m$^2$ (median: 30 stems per m$^2$).

## 3.3 | Statistical models

Results of model 1 using the presence or absence of Japanese knotweed as the binary independent variable are detailed in Table 3. According to this model, which has a $R^2$ of 0.248, in 2019, there were nearly 3 cm more erosion (coefficient $= -2.81$) where knotweed was present than where it was absent, a significant difference ($p = .046$). This difference was probably amplified by the fact that sites with knotweed also seemed to accumulate less sediments than sites without.

The slope seemed to have accentuated erosion (coefficient $= -15.99$), although the significance level for this variable was slightly above 0.05 ($p = .055$). Being on an islet significantly influenced erosion ($p = .003$); in 2019, there were 10 cm more erosion (coefficient $= -10.03$) on islets than on linear riverbanks. The model also indicated that fixed effects of location influenced erosion, that is, the extent of erosion varied depending where the data were collected. Even taking these additional factors into account, the model indicated that this variability does not mask the effect of knotweed on erosion, which is therefore presumed, statistically speaking, real. Results of the two additional models, each run with half the sample, were almost identical to those of the base model, suggesting that model 1was robust.

Results of model 2, which used Japanese knotweed stem density as a continuous independent variable, are detailed in Table 4. According to this model, which has a $R^2$ of 0.265, the higher the stem density, the greater the erosion in 2019 (coefficient $= -0.067$), even after accounting for the fixed effects of location. Thus, for each 10-fold increase in stem density, an additional 0.67 cm of soil was lost. This effect is significant ($p = .004$). The influence of slope or being on an islet is similar in models 1 and 2. Results of the two additional models, each run with half the sample, were nearly identical to those of the base model, suggesting that model 2 was robust.

**TABLE 1** Proportion of vegetation survey points belonging to each vegetation class for each of the four types of riverbank along the Etchemin River (Québec, Canada)

| | Vegetation class | |
|---|---|---|
| Riverbank morphology | Japanese knotweed (% vegetation survey points) | Other vegetation (% vegetation survey points) |
| Concave | 51% | 49% |
| Convex | 50% | 50% |
| Linear | 23% | 77% |
| Islet | 61% | 39% |

# 4 | DISCUSSION

Statistical models built with elevation change data collected on the riverbanks of the Etchemin River, some invaded by Japanese knotweed and others not, suggest that the invaded riverbanks are more vulnerable to erosion than those which are not invaded. Invaded

**TABLE 2** Vascular plant species associated with vegetation survey points with or without Japanese knotweed, on the riverbanks of the Etchemin River (Québec, Canada)

| With Japanese knotweed | | Without Japanese knotweed | |
|---|---|---|---|
| Species | *n* sampling points with the species | Species | *n* sampling points with the species |
| *Reynoutria japonica* Houttuyn | 764 | *Phalaris arundinacea* Linnaeus | 845 |
| *Phalaris arundinacea* Linnaeus | 95 | Poaceae spp. | 433 |
| *Acer negundo* Linnaeus | 90 | *Equisetum arvense* Linnaeus | 264 |
| *Salix* ×*fragilis* Linnaeus | 78 | *Bromus inermis* Leysser | 222 |
| *Apios americana* Medikus | 61 | *Apios americana* Medikus | 107 |
| Poaceae spp. | 57 | *Calystegia sepium* (Linnaeus) R. Brown | 77 |
| *Echinocystis lobata* (Michaux) Torrey & A. gray | 46 | *Onoclea sensibilis* Linnaeus | 70 |
| *Matteuccia struthiopteris* (Linnaeus) Todaro | 45 | *Clematis virginiana* Linnaeus | 49 |
| *Calystegia sepium* (Linnaeus) R. Brown | 29 | *Carex* spp. | 48 |
| *Equisetum arvense* Linnaeus | 22 | *Salix eriocephala* Michaux | 46 |

*Note*: Only the 10 most frequently sampled species (or group of species) are indicated.

**TABLE 3** Multiple regression model testing the effect of Japanese knotweed on elevation changes (2019 vs. 2018) of the riverbanks of the Etchemin River (Québec, Canada) and whose binary independent variable is the presence or absence of knotweed

| Variable | | Coefficient | Standard error | $t$ | $p$ | 95% confidence interval | | Sig.[a] |
|---|---|---|---|---|---|---|---|---|
| Presence of Japanese knotweed | | −2.808 | 1.246 | −2.25 | .046 | −5.551 | −0.065 | ** |
| Soil textural class (vs. sandy loam) | Sandy loam | 3.308 | 3.346 | 0.99 | .344 | −4.056 | 10.671 | |
| | Loam | 5.057 | 2.803 | 1.80 | .099 | −1.112 | 11.226 | * |
| Slope | | −15.993 | 7.449 | −2.15 | .055 | −32.387 | 0.401 | * |
| Riverbank morphology (vs. linear) | Convex | −4.069 | 4.043 | −1.01 | .336 | −12.967 | 4.830 | |
| | Concave | 0.515 | 2.500 | 0.21 | .841 | −4.987 | 6.017 | |
| | Islet | −10.032 | 2.703 | −3.71 | .003 | −15.982 | −4.082 | *** |
| Distance from the river (water) | | −0.333 | 0.218 | −1.53 | .155 | −0.814 | 0.147 | |

*Note*: The $R^2$ of the model is 0.248.
[a]Significance:****p* < .01, ***p* < .05, **p* < .10.

**TABLE 4** Multiple regression model testing the effect of Japanese knotweed stem density on elevation changes (2019 vs. 2018) of the riverbanks of the Etchemin River (Québec, Canada)

| Variables | | Coefficient | Standard error | $t$ | $p$ | 95% confidence interval | | Sig.[a] |
|---|---|---|---|---|---|---|---|---|
| Japanese knotweed stem density | | −0.067 | 0.019 | −3.59 | .004 | −0.109 | −0.026 | *** |
| Soil textural class (vs. sandy loam) | Sandy loam | 2.784 | 3.160 | 0.88 | .397 | −4.172 | 9.740 | |
| | Loam | 4.682 | 2.793 | 1.68 | .122 | −1.465 | 10.828 | |
| Slope | | −16.000 | 7.485 | −2.14 | .056 | −32.475 | 0.475 | * |
| Riverbank morphology (vs. linear) | Convex | −4.473 | 4.111 | −1.09 | .300 | −13.521 | 4.576 | |
| | Concave | −0.549 | 2.536 | −0.22 | .833 | −6.132 | 5.033 | |
| | Islet | −10.885 | 2.440 | −4.46 | .001 | −16.254 | −5.515 | *** |
| Distance from the river | | −0.422 | 0.196 | −2.16 | .054 | −0.854 | 0.009 | * |

*Note*: The $R^2$ of the model is 0.265.
[a]Significance:****p* < .01, ***p* < .05, **p* < .10.

riverbanks lost between surveys about 3 cm more soil than banks without knotweed. Higher knotweed stem density, steeper riverbanks, and being on an islet also favored increased soil loss.

This greater vulnerability to erosion in the presence of Japanese knotweed can be explained as follows. Dead knotweed stems are evacuated by water and ice flow during the spring flood. Denuded of their vegetation, the riverbanks are no longer protected from scouring by water and ice. Moreover, the absence of vegetation reduces the roughness of the riverbank, accelerating runoff and increasing its erosive force (Hopkinson & Wynn, 2009; Thorne & Furbish, 1995). Although knotweed has a large underground biomass, the rhizomes do not prevent soil surface erosion, nor compensate for the loss of aerial plant structures, which are no longer present to trap sediments (Colleran et al., 2020).

This additional erosion of nearly 3 cm is equivalent to a soil loss of 25–45 kg m$^{-2}$ per spring flooding episode given the bulk density of sandy loams and loamy sands, which varies from 0.9 (Saint-Laurent, Gervais-Beaulac, Paradis, Arsenault-Boucher, & Demers, 2017) to 1.6 tons m$^{-3}$ (Alberta Agriculture and Rural Development, 2010). In comparison, purple jewelweed (*Impatiens glandulifera*), another riverside invasive species, may occasionally cause soil losses of 3–17 kg m$^{-2}$ per winter (6 months) along Swiss and English rivers (Greenwood et al., 2018). For a highly invaded river such as the Etchemin at Saint-Henri-de-Lévis, soil losses from Japanese knotweed may be important. In 2018, knotweed clones covered 119,000 m$^2$ of riverbank along a 23-km stretch located upstream to the village (Matte, 2020). Our results indicate that these clones may have caused, in 2019, an additional soil loss of 3,000–5,330 tons. This value must however be put into context. In this agricultural region where the shrub cover of most riverbanks has been removed, the average soil erosion would be nearly 2 cm, even without knotweed. This represents an estimated soil loss of 15–27 kg m$^{-2}$, and thus between 1,820 and 3,240 tons of soil over 119,000 m$^2$. Notwithstanding, the additional erosion caused by knotweed remained considerable (+92% to +290%).

Some conditions along the river further accentuate the effect of Japanese knotweed on erosion. A riverbank invaded with knotweed and with a steep slope will be more eroded because steeper banks allow faster water flow than flatter banks (Krzeminska, Kerkhof, Skaalsveen, & Stolte, 2019; Laubel, Kronvang, Hald, & Jensen, 2003; Zhao et al., 2020). Islets in invaded rivers are particularly susceptible to erosion because they are completely submerged during flooding. They are also directly in the path of ice during mechanical ice breakup.

The study period, which spanned November 2018–June 2019, was marked by an exceptionally strong spring flood with a recurrence interval of nearly 50 years and by two mechanical ice breakups. It is therefore likely that the estimated soil loss recorded in 2019 was exceptional. Given the highly variable nature of flood intensity from year to year, it would be important to study the impact of Japanese knotweed on fluvial geomorphology over a longer period. Longitudinal studies would better document the extent of soil losses caused by the invader and whether these losses significantly increase sedimentation of rivers or lakes. Should this be the case, the integrity of aquatic ecosystems could be impaired by the large amount of waterborne sediments. Increased water temperature, decreased dissolved oxygen, spawning bed siltation, inflammation of fish gills, and pollution by pesticides and fertilizers leached with the eroded sediments could result from increased knotweed occupation along river environment (Greig, Sear, & Carling, 2005; Mol & Ouboter, 2004; Österling, 2015; Paaijmans, Takken, Githeko, & Jacobs, 2008; Reash & Berra, 1989).

Projections of climate change effects over the next 30 years in southern Québec predict earlier (by 22–34 days) but less voluminous spring floods due to a warmer climate and a thinner snow cover (Boyer, Chaumont, Chartier, & Roy, 2010). On the other hand, summer, autumn, and winter floods with higher peak discharges could become more frequent (Ouranos, 2015), leaving riverbanks invaded by Japanese knotweed more vulnerable to erosion during these periods. In some rivers, the more frequent floods in winter could cause recurring ice breakups and ice jams (Morse & Turcotte, 2018). This could contribute to further erode banks with knotweed clones and to generate a higher number of rhizome fragments that will accelerate the invasion process. Combined to a probable expansion of knotweed populations caused by climate warming (Groeneveld, Belzile, & Lavoie, 2014), the future impact of this invader on riverbank dynamics should not be underestimated.

## ACKNOWLEDGMENTS

This research was financially supported by the Natural Sciences and Engineering Research Council of Canada (grant to Claude Lavoie: 2018-03715) and the Fonds de recherche du Québec Nature et Technologies (grant to Maxime Boivin: 253035; scholarship to Rébecca Matte). The authors thank Marianne Bouchard, Elisabeth Groeneveld, and Maxime Maltais for field assistance, Diego Andres Cardenas Morales and Jean Dubé for help with statistical analyses, Elisabeth Groeneveld for the English translation of the manuscript, and two anonymous reviewers for comments.

## CONFLICT OF INTEREST

The authors declare no conflicts of interest.

## DATA AVAILABILITY STATEMENT

The data that support the findings of this study are openly available in Scholars Portal Dataverse at https://dataverse.scholarsportal.info/dataverse/laval.

## ORCID

*Maxime Boivin* https://orcid.org/0000-0002-1248-8061
*Claude Lavoie* https://orcid.org/0000-0001-6510-5178

## REFERENCES

Alberta Agriculture and Rural Development. (2010). *Agricultural soil compaction: Causes and management* (p. 10). Edmonton, Canada: Alberta Agriculture and Rural Development.

Arnold, E., & Toran, L. (2018). Effects of bank vegetation and incision on erosion rates in an urban stream. *Water*, *10*(4), 482. https://doi.org/10.3390/w10040482

Bankhead, N. L., Thomas, R. E., & Simon, A. (2017). A combined field, laboratory and numerical study of the forces applied to, and the potential for removal of, bar top vegetation in a braided river. *Earth Surface Processes and Landforms*, *42*(3), 439–459. https://doi.org/10.1002/esp.3997

Bartley, R., Keen, R. J., Hawdon, A. A., Hairsine, P. B., Disher, M. G., & Kinsey-Henderson, A. E. (2008). Bank erosion and channel width change in a tropical catchment. *Earth Surface Processes and Landforms*, *33*(14), 2174–2200. https://doi.org/10.1002/esp.1678

Birkeland, G. H. (1996). Riparian vegetation and sandbar morphology along the lower little Colorado River, Arizona. *Physical Geography*, *17*(6), 534–553. https://doi.org/10.1080/02723646.1996.10642600

Booth, D. B. (1990). Stream-channel incision following drainage-basin urbanization. *Journal of the American Water Resources Association*, *26*(3), 407–417. https://doi.org/10.1111/j.1752-1688.1990.tb01380.x

Bouyoucos, G. J. (1962). Hydrometer method improved for making particle size analyses of soils. *Agronomy Journal*, *54*(5), 464–465. https://doi.org/10.2134/agronj1962.00021962005400050028x

Boyer, C., Chaumont, D., Chartier, I., & Roy, A. G. (2010). Impact of climate change on the hydrology of St. Lawrence tributaries. *Journal of Hydrology*, *384*(1–2), 65–83. https://doi.org/10.1016/j.jhydrol.2010.01.011

Child, L., & Wade, M. (2000). *The Japanese knotweed manual* (p. 123). Chichester, England: Packard Publishing Limited.

Colleran, B., Lacy, S. N., & Retamal, M. R. (2020). Invasive Japanese knotweed (*Reynoutria japonica* Houtt.) and related knotweeds as catalysts for streambank erosion. *River Research and Applications*, *36*(9), 1962–1969. https://doi.org/10.1002/rra.3725

Conseil de bassin de la rivière Etchemin. (2014). Plan directeur de l'eau des bassins versants des secteurs d'intervention de la Zone Etchemin. Version finale. Saint-Henri-de-Lévis, Canada: Conseil de bassin de la rivière Etchemin, 333p.

Corenblit, D., Baas, A. C. W., Bornette, G., Darrozes, J., Delmotte, S., Francis, R. A., … Steiger, J. (2011). Feedbacks between geomorphology and biota controlling earth surface processes and landforms: A review of foundation concepts and current understandings. *Earth-Science Reviews*, *106*(3–4), 307–331. https://doi.org/10.1016/j.earscirev.2011.03.002

Davies, N. S., & Gibling, M. R. (2009). Cambrian to Devonian evolution of alluvial systems: The sedimentological impact of the earliest land plants. *Earth-Science Reviews*, *98*(3–4), 171–200. https://doi.org/10.1016/j.earscirev.2009.11.002

Davies, N. S., & Gibling, M. R. (2010). Paleozoic vegetation and the Siluro-Devonian rise of fluvial lateral accretion sets. *Geology*, *38*(1), 51–54. https://doi.org/10.1130/G30443.1

Dietrich, J. T. (2014). Applications of structure-from-motion photogrammetry to fluvial geomorphology. A doctoral dissertation in pursuit of a Geography degree from the University of Oregon. Retrieved from https://scholarsbank.uoregon.edu/xmlui/handle/1794/18701

Duró, G., Crosato, A., Kleinhans, M. G., & Uijttewaal, W. S. J. (2018). A low-cost technique to measure bank erosion processes along middle-size river reaches. *Earth Surface Dynamics Discussions*, *6*, 933–953. https://doi.org/10.5194/esurf-2018-3

Environnement Canada. (2021). Données des stations pour le calcul des normales climatiques au Canada de 1981 à 2010: Beauséjour. Retrieved from https://climat.meteo.gc.ca/climate_normals/results_1981_2010_f.html?searchType=stnName&txtStationName=Beaus%C3%A9jour&searchMethod=contains&txtCentralLatMin=0&txtCentralLatSec=0&txtCentralLongMin=0&txtCentralLongSec=0&stnID=5315&dispBack=0

ESRI. (2018). *ArcGIS Desktop, version 10.6*. Redlands, CA: Environmental Systems Research Institute.

Foucher, A., Salvador-Blanes, S., Vandromme, R., Cerdan, O., & Desmet, M. (2017). Quantification of bank erosion in a drained agricultural lowland catchment. *Hydrological Processes*, *31*(6), 1424–1437. https://doi.org/10.1002/hyp.11117

Graf, W. L. (1978). Fluvial adjustments to the spread of tamarisk in the Colorado plateau region. *Geological Society of America Bulletin*, *89*(10), 1491–1501.

Greenwood, P., Baumann, P., Pulley, S., & Kuhn, N. J. (2018). The invasive alien plant, *Impatiens glandulifera* (Himalayan balsam), and increased soil erosion: Causation or association? Case studies from a river system in Switzerland and the UK. *Journal of Soils and Sediments*, *18*(12), 3463–3477. https://doi.org/10.1007/s11368-018-2041-0

Greenwood, P., Gange, A. C., & Kuhn, N. J. (2020). Evidence of sedimentation inequality along riparian areas colonised *by Impatiens glandulifera* (Himalayan balsam). *Weed Research*, *60*(1), 26–36. https://doi.org/10.1111/wre.12397

Greenwood, P., & Kuhn, N. J. (2014). Does the invasive plant, *Impatiens glandulifera*, promote soil erosion along the riparian zone? An investigation on a small watercourse in Northwest Switzerland. *Journal of Soils and Sediments*, *14*(3), 637–650. https://doi.org/10.1007/s11368-013-0825-9

Greig, S. M., Sear, D. A., & Carling, P. A. (2005). The impact of fine sediment accumulation on the survival of incubating salmon progeny: Implications for sediment management. *Science of the Total Environment*, *344*(1–3), 241–258. https://doi.org/10.1016/j.scitotenv.2005.02.010

Groeneveld, E., Belzile, F., & Lavoie, C. (2014). Sexual reproduction of Japanese knotweed (*Fallopia japonica* s.l.) at its northern distribution limit: New evidence of the effect of climate warming on an invasive species. *American Journal of Botany*, *101*(3), 459–466. https://doi.org/10.3732/ajb.1300386

Gurnell, A. M., Holloway, J. V., Liffen, T., Serlet, A. J., & Zolezzi, G. (2018). Plant root and rhizome strength: Are there differences between and within species and rivers? *Earth Surface Processes and Landforms*, *44*(1), 389–392. https://doi.org/10.1002/esp.4499

Harmel, R. D., Haan, C. T., & Dutnell, R. (1999). Bank erosion and riparian vegetation influences: Upper Illinois River, Oklahoma. *Transactions of the American Society of Agricultural Engineers*, *42*(5), 1321–1330. https://doi.org/10.13031/2013.13295

Hopkinson, L., & Wynn, T. (2009). Vegetation impacts on near bank flow. *Ecohydrology*, *2*(4), 404–418. https://doi.org/10.1002/eco.87

Invasive Species Specialist Group (2016). *Polygonum cuspidatum*. Retrieved from http://www.iucngisd.org/gisd/species.php?sc=91

Keim, F. D., Beadle, G. W., & Frolik, A. L. (1932). The identification of the more important prairie hay grasses of Nebraska by their vegetative characters. Lincoln, NE: University of Nebraska, College of Agriculture, Agricultural Experiment Station Research Bulletin. *65*, 40.

Krzeminska, D., Kerkhof, T., Skaalsveen, K., & Stolte, J. (2019). Effect of riparian vegetation on stream bank stability in small agricultural catchments. *Catena*, *172*, 87–96. https://doi.org/10.1016/j.catena.2018.08.014

Laubel, A., Kronvang, B., Hald, A. B., & Jensen, C. (2003). Hydromorphological and biological factors influencing sediment and phosphorus loss via bank erosion in small lowland rural streams in Denmark. *Hydrological Processes*, *17*(17), 3443–3463. https://doi.org/10.1002/hyp.1302

Lavoie, C. (2017). The impact of invasive knotweed species (*Reynoutria* spp.) on the environment: Review and research perspectives. *Biological Invasions*, *19*(8), 2319–2337. https://doi.org/10.1007/s10530-017-1444-y

Lavoie, C. (2019). *50 plantes envahissantes: Protéger la nature et l'agriculture* (p. 416). Québec, Canada: Les Publications du Québec.

Lawler, D. M. (1993). The measurement of river bank erosion and lateral channel change: A review. *Earth Surface Processes and Landforms*, *18*(9), 777–821. https://doi.org/10.1002/esp.3290180905

Matte, R. (2020). Crues, dissémination et impact de la renouée du Japon en milieux riverains. A master's Thesis in Pursuit of an Aménagement du Territoire et développement régional Degree from Université Laval. Retrieved from https://corpus.ulaval.ca/jspui/bitstream/20.500.11794/67009/1/36671.pdf

Meier, C. I., Reid, B. L., & Sandoval, O. (2013). Effects of the invasive plant *Lupinus polyphyllus* on vertical accretion of fine sediment and nutrient availability in bars of the gravel-bed Paloma river. *Limnologica*, *43*(5), 381–387. https://doi.org/10.1016/j.limno.2013.05.004

Michigan Department of Natural Resources. (2012). Japanese knotweed. Retrieved from https://www.michigan.gov/documents/dnr/knotweed_BCP_372280_7.pdf

Microsoft. (2016). *Excel*. Redmond, WA: Microsoft Corporation.

Ministère de l'Énergie et des Ressources naturelles du Québec. (2015). *Mosaïque d'orthophotographies de Chaudière-Appalaches – 2015 (30 cm)*. Québec, Canada: Ministère de l'Énergie et des Ressources naturelles du Québec.

Ministère de l'Environnement et de la Lutte contre les changements climatiques du Québec. (2020). Station 023303. Etchemin – au pont-route 173 à Saint-Henri-de-Lévis. Retrieved from https://www.cehq.gouv.qc.ca/depot/historique_donnees/fichier/023303_Q.txt

Mol, J. H., & Ouboter, P. E. (2004). Downstream effects of erosion from small-scale gold mining on the instream habitat and fish community of a small neotropical rainforest stream. *Conservation Biology*, *18*(1), 201–214. https://doi.org/10.1111/j.1523-1739.2004.00080.x

Morse, B., & Turcotte, B. (2018). *Risque d'inondations par embâcles de glaces et estimation des débits hivernaux dans un contexte de changements climatiques (volet A)* (p. 79p). Québec, Canada: Université Laval.

Mummigatti, K. (2008). The effects of Japanese Knotweed (*Reynoutria japonica*) on riparian lands in Otsego County, New York. Retrieved from https://www.oneonta.edu/academics/biofld/PUBS/ANNUAL/2007/Effects%20of%20Knotweed%20growth.pdf

Murray, A. B., Knaapen, M. A. F., Tal, M., & Kirwan, M. L. (2008). Biomorphodynamics: Physical-biological feedbacks that shape landscapes. *Water Resources Research*, *44*(11), W11301. https://doi.org/10.1029/2007WR006410

Murray, A. B., & Paola, C. (2003). Modeling the effect of vegetation on channel pattern in bedload rivers. *Earth Surface Processes and Landforms*, *28*(2), 131–143. https://doi.org/10.1002/esp.428

Österling, E. M. (2015). Timing, growth and proportion of spawners of the threatened unionoid mussel *Margaritifera margaritifera*: Influence of water temperature, turbidity and mussel density. *Aquatic Sciences*, *77*(1), 1–8. https://doi.org/10.1007/s00027-014-0366-3

Ouranos. (2015). *Vers l'adaptation. Synthèse des connaissances sur les changements climatiques au Québec. Édition 2015* (p. 415). Montréal, Canada: Ouranos.

Paaijmans, K. P., Takken, W., Githeko, A. K., & Jacobs, A. F. G. (2008). The effect of water turbidity on the near-surface water temperature of larval habitats of the malaria mosquito *Anopheles gambiae*. *International Journal of Biometeorology*, *52*(8), 747–753. https://doi.org/10.1007/s00484-008-0167-2

Reash, R. J., & Berra, T. M. (1989). Incidence of fin erosion and anomalous fishes in a polluted stream and a nearby clean stream. *Water, Air, and Soil Pollution*, *47*(1), 47–63. https://doi.org/10.1007/BF00468996

Rowntree, K. (1991). An assessment of the potential impact of alien invasive vegetation on the geomorphology of river channels in

South Africa. *Southern African Journal of Aquatic Sciences*, *17*(1–2), 28–43. https://doi.org/10.1080/10183469.1991.9631311

Saint-Laurent, D., Gervais-Beaulac, V., Paradis, R., Arsenault-Boucher, L., & Demers, S. (2017). Distribution of soil organic carbon in riparian forest soils affected by frequent floods (southern Québec, Canada). *Forests*, *8*(4), 124. https://doi.org/10.3390/f8040124

Schumm, S. A. (1968). Speculations concerning paleohydrologic controls of terrestrial sedimentation. *Geological Society of America Bulletin*, *79*(11), 1573–1588. https://doi.org/10.1130/0016-7606

Simon, A., & Collison, A. J. C. (2002). Quantifying the mechanical and hydrologic effects of riparian vegetation on streambank stability. *Earth Surface Processes and Landforms*, *27*(5), 527–546. https://doi.org/10.1002/esp.325

Smith, D. G. (1976). Effect of vegetation on lateral migration of anastomosed channels of a glacier meltwater river. *Geological Society of America Bulletin*, *87*(6), 857–860. https://doi.org/10.1130/0016-7606

StataCorp. (2016). *Stata 14.2*. College Station, TX: StataCorp LLC.

Stover, J. E., Keller, E. A., Dudley, T. L., & Langendoen, E. J. (2018). Fluvial geomorphology, root distribution, and tensile strength of the invasive giant reed, *Arundo donax* and its role on stream bank stability in the Santa Clara River, Southern California. *Geosciences*, *8*(8), 304. https://doi.org/10.3390/geosciences8080304

Thorne, S. D., & Furbish, D. J. (1995). Influences of coarse bank roughness on flow within a sharply curved river bend. *Geomorphology*, *12*(3), 241–257. https://doi.org/10.1016/0169-555X(95)00007-R

Tickner, D. P., Angold, P. G., Gurnell, A. M., & Mountford, J. O. (2001). Riparian plant invasions: Hydrogeomorphical control and ecological impacts. *Progress in Physical Geography*, *25*(1), 22–52. https://doi.org/10.1177/030913330102500102

Van de Wiel, M. J., & Darby, S. E. (2007). A new model to analyse the impact of woody riparian vegetation on the geotechnical stability of riverbanks. *Earth Surface Processes and Landforms*, *32*(14), 2185–2198. https://doi.org/10.1002/esp.1522

van Oorschot, M., Kleinhans, M. G., Geerling, G. W., Egger, G., Leuven, R. S. E. W., & Middelkoop, H. (2017). Modeling invasive alien plant species in river systems: Interaction with native ecosystem engineers and effects on hydro-morphodynamic processes. *Water Resources Research*, *53*(8), 6945–6969. https://doi.org/10.1002/2017WR020854

White, H. (1980). A heteroskedasticity-consistent covariance matrix estimator and a direct test for heteroskedasticity. *Econometrica*, *48*(4), 817–838. https://doi.org/10.2307/1912934

Zhao, J., Zhang, H., Yang, C., Lee, L. M., Zhao, X., & Lai, Q. (2020). Experimental study of reservoir bank collapse in gravel soil under different slope gradients and water levels. *Natural Hazards*, *102*(1), 249–273. https://doi.org/10.1007/s11069-020-03922-z

Zhu, H., Hu, X., Li, Z., Song, L., Li, K., Li, X., & Li, G. (2018). The influences of riparian vegetation on bank failures of a small meadow-type meandering river. *Water*, *10*(6), 692. https://doi.org/10.3390/w10060692

Ziliani, L., & Surian, N. (2012). Evolutionary trajectory of channel morphology and controlling factors in a large gravel-bed river. *Geomorphology*, *173–174*, 104–117. https://doi.org/10.1016/j.geomorph.2012.06.001

**How to cite this article:** Matte, R., Boivin, M., & Lavoie, C. (2022). Japanese knotweed increases soil erosion on riverbanks. *River Research and Applications*, *38*(3), 561–572. https://doi.org/10.1002/rra.3918